Thermoelastoplastic and Residual Stress Analysis during Induction Hardening of Steel

S. Jahanian

A theoretical model was developed to predict the thermoelastoplastic and residual stresses developed in a round steel bar during induction hardening. For numerical analysis, a quasi-static, uncoupled thermoelastoplastic solution based on the hyperbolic sine law of Tien and Richmond was formulated. The properties of the material were assumed to be temperature dependent. The phase transformation was considered in the numerical calculation, and the results were compared with the case where phase transformation is avoided. The cylinder was heated rapidly; once the temperature of the outer surface exceeded the transformation temperature, the cylinder was rapidly cooled. Accordingly, in the numerical calculation, only the area at the vicinity of the outer surface was assumed to transform to martensite. The results showed that the compressive residual stresses at the vicinity of the outer surface were considerably higher than the tensile stresses at the center.

Keywords

induction hardening, induction hardening stresses, modeling, residual stress, stress (residual) calculations

1. Introduction

THE DEVELOPMENT of beneficial residual stress distribution in the surface of steel can be achieved by rapidly heating only the surface layers to the austenite region, followed by rapid cooling of those layers to room temperature. Induction hardening is a common practice in industry—particularly for long shafts—which results in the development of compressive residual stresses at the outer surface of the cylinder. During induction hardening of round bars, the bar is rapidly heated to a temperature above its critical temperature by inductors. Later, quench rings are used to quench the bar rapidly. Due to the formation of martensite at the outer surface of the bar, compressive residual stresses are developed, particularly at the surface. Determination of these stresses is an important factor in design. The objective of this paper is to introduce a combined analytical and numerical method for determination of the residual and thermoelastoplastic stresses during this process.

A survey of the literature shows that the problem of thermoelastoplastic and residual stress distribution in quenched bodies has attracted numerous researchers. While it is not our intention to discuss all the work that has been done in this field, we will review key papers. The earliest analysis of quenching problems dates back to the late 1920s, when Sachs (Ref 1) presented his classic work in this branch of science. Weiner et al. (Ref 2, 3) were among the first investigators who looked into more complex types of transient thermoelastoplastic problems. Later, these types of problems were investigated by several other researchers (Ref 4-11).

Extension of the method of successive elastic solution developed by Mendelson (Ref 12) has been adopted by several investigators (Ref 13-20). Ishikawa et al. (Ref 13-16) solved the problem for the Ramberg-Osgood type of material, and Jahanian et al. (Ref 17-20) extended the Mendelson method for a material of linear strain hardening. The thermal stresses that are developed during the phase transformation have been addressed in Ref 16, 21, and 22.

The present research considers the problem of transient thermal stress in an infinitely long solid cylinder of low-carbon steel with nonlinear strain hardening and temperature-dependent properties. The cylinder is heated rapidly to 840 °C, which is above the transformation temperature. Then it is cooled rapidly. Thermoelastoplastic modeling uses the hyperbolic sine law of Tien and Richmond (Ref 23). In numerical modeling, martensitic transformation during cooling and transformation of α-iron to γ-iron during heating were carefully examined.

2. Theoretical Analysis

A low-carbon solid cylinder of radius a is considered. At $t = 0$, this cylinder is assumed to be at a uniform temperature of T_0. At $t > 0$, the outside of the cylinder is heated by an instantaneous

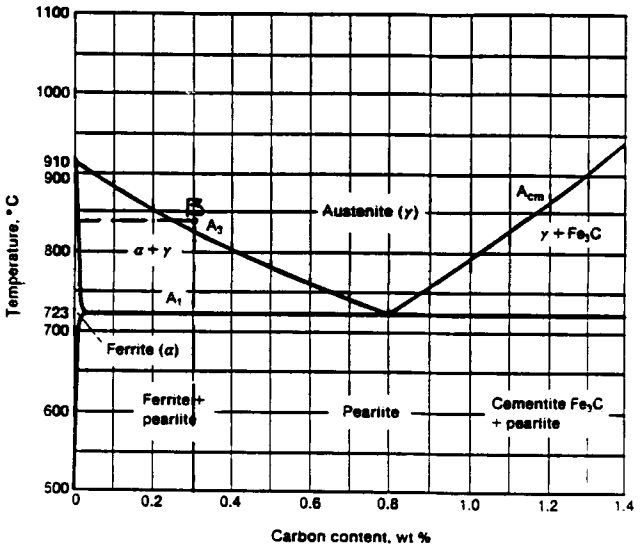

Fig. 1 Lower left-hand portion of the iron-carbon phase diagram. Source: Ref 24

S. Jahanian, Department of Mechanical Engineering Technology, Pennsylvania State University, Altoona, PA 16602, USA.

increase in the temperature of the medium to a value of T_f, which is assumed to be above the transformation temperature. Following heating over a period of τ, the cylinder is instantaneously cooled to its original temperature, T_0. This research deals with the thermoelastoplastic stress analysis of such a cylinder. This is done by considering A_1 and A_3 phase transformation on heating (Fig. 1) and martensitic transformation on cooling (Fig. 2).

2.1 *Metallurgical Response*

Consider a cylinder that is rapidly heated to a temperature above A_3 and then rapidly cooled. From a metallurgical point of view, carbon steel expands regularly while being heated to T_{A_1} and then contracts to T_{A_3}. During heating through the range T_{A_1} to T_{A_3}, α-iron transforms to γ-iron and iron carbide goes into solution in γ-iron. At T_{A_3}, the steel resumes its expansion.

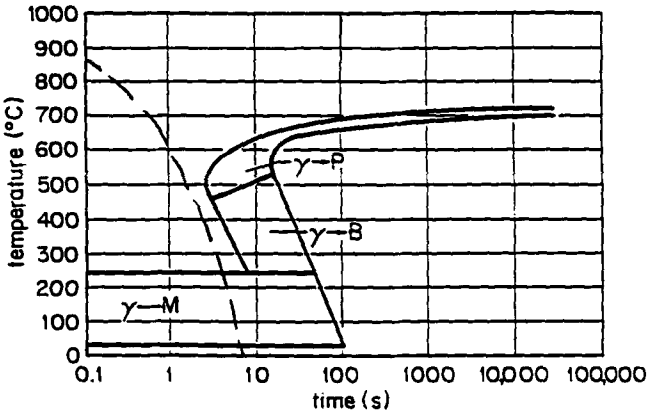

Fig. 2 Continuous cooling transformation diagram. Dashed line: martensitic transformation. Source: Ref 25

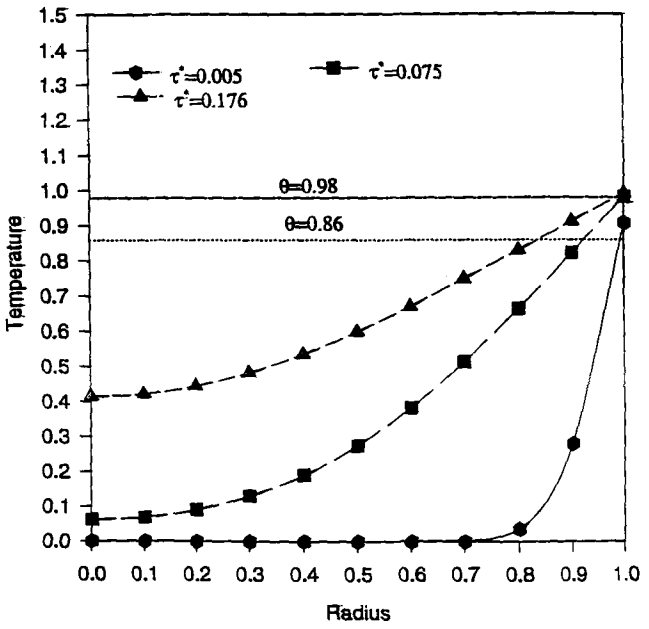

Fig. 3 Temperature distribution during rapid heating

On cooling, martensitic transformation—particularly martensitic pearlite transformation—or pearlitic transformation occurs, depending on the cooling rate. It should be pointed out that the transformation during cooling depends on the relation between the real time, temperature, and, obviously, rate of cooling. If the rate of cooling is high enough and uniform, only martensitic transformation occurs. In the problem in question, the temperature of the cylinder at the vicinity of its outside surface remains above A_3 for a short period of time (T_f = 840 °C). The thickness of this region is very small. Accordingly, during cooling only the very small portion of the cylinder that is at the vicinity of the outside surface will completely transform to martensite. The rest of the cylinder will not have enough time during heating to exceed the transformation temperature (see Fig. 3 and 4).

2.2 *Transient Temperature Distribution*

The transient temperature distribution in the cylinder can be found by solving the general heat conduction equation (Ref 26):

$$\text{div}[K(\text{grad}T)] = \gamma C \frac{\partial T}{\partial t} \qquad \text{(Eq 1)}$$

where K is thermal conductivity, C is specific heat, and γ is mass density They are defined by two parameters: The first, designated by zero, is the dimensional part; the second is the temperature-dependent part:

$$K = K_0 K^*(\theta), \ldots C = C_0 C^*(\theta)$$
$$\gamma = \gamma_0 \gamma^*(\theta) \qquad \text{(Eq 2)}$$

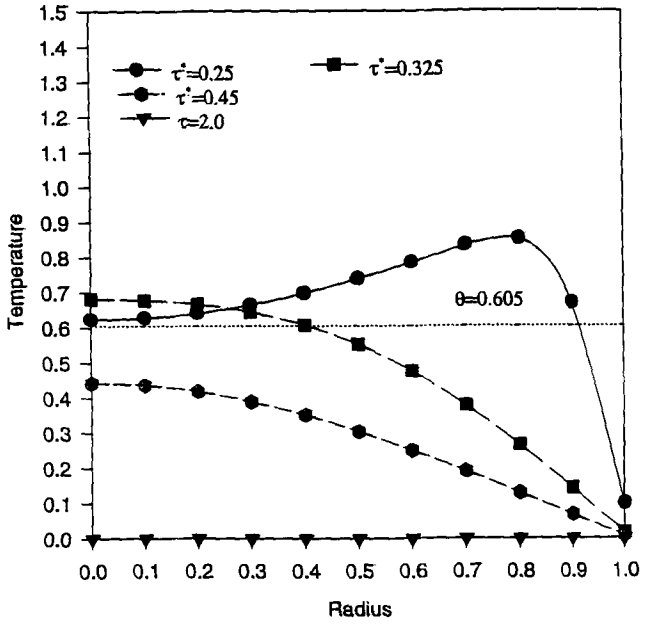

Fig. 4 Temperature distribution during rapid cooling

The solution of such a problem when the cylinder is heated to temperature T_f could be obtained as follows (Ref 26):

$$\theta(\rho,\tau) = \frac{1}{K_1}[1 - (1 - 2K_1\phi)^{1/2}] \quad \text{(Eq 3)}$$

where

$$\phi = 2\beta_h\phi_0 \sum_{m=1}^{\infty} e^{-\lambda_n^2\tau} \frac{J_0(\lambda_n r)}{(\lambda_n^2 a^2 + \beta_h^2)J_0(\lambda_n a)} \quad \text{(Eq 3a)}$$

and K_1 is a dimensionless parameter defined as:

$$K^*(\theta) = 1 - K_1\theta \quad \text{(Eq 3b)}$$

In the previous equations:

$$\phi_0 = 1 - \frac{K_1}{2},\ \beta_h = \frac{ah}{K_0},\ s = \frac{K_0}{\gamma_0 c_0 a^2}\, t,$$

$$\lambda_n = \frac{\alpha_n}{a},\ h^* = \frac{K^*}{C^*\gamma^*},\ \tau = h^* s,\ \theta = \frac{T_f - T}{T_f - T_0} \quad \text{(Eq 4)}$$

where α_n can be found by solving:

$$\alpha_n J_1(\alpha_n) - \beta_h J_0(\alpha_n) = 0 \quad \text{(Eq 4a)}$$

β_h is the Biot number during heating, and the boundary conditions are:

$$\frac{\partial\theta_1}{\partial r}(0,\tau) = 0$$

$$-K\frac{\partial\theta_1}{\partial r}(R,\tau) = h_1[\theta_1(R,\tau)] \quad \text{(Eq 5)}$$

During the cooling part of the cycle for $\tau \geq \tau_1$, the initial boundary conditions are:

$$\theta = \theta_2(r,\tau)$$

$$\frac{\partial\theta_2}{\partial r}(0,\tau) = 0$$

$$-K\frac{\partial\theta_2}{\partial r}(R,\tau) = h_2[\theta_2(R,\tau)]$$

$$\theta_2(r,0) = \theta_1(r,\tau_1) \quad \text{(Eq 5a)}$$

Introducing the above boundary conditions to Eq 1 leads to:

$$\theta_2 = \frac{1}{K_1}[1 - (1 - 2K_1\phi_2)^{1/2}] \quad \text{(Eq 6)}$$

where:

$$\phi_2 = \phi_0 \sum_{m=1}^{\infty} b_n e^{-\gamma_n^2(\tau - \tau_1)} J_0(\gamma_n r) \qquad \tau > \tau_1 \quad \text{(Eq 6a)}$$

and

$$b_n = \frac{1}{N_n}\left[\frac{J_1(\gamma_n)}{\gamma_n} - 2\beta_h \sum_{m=1}^{\infty} C_m Q_{mn}\right]$$

$$N_n = \frac{\gamma_n^2 + \beta_c^2}{2\gamma_n^2} J_0^2(\gamma_n) \quad \text{(Eq 6b)}$$

$$C_m = \frac{e^{-\lambda_m^2\tau_1}}{(\lambda_m^2 + \beta_h^2)J_0(\lambda_m)}$$

$$Q_{mn} = \frac{(\beta_c - \beta_h)J_0(\gamma_m)J_0(\lambda_n)}{\gamma_m^2 - \lambda_n^2} \quad \text{(Eq 6c)}$$

where:

$$\beta_c = Rh_c/K$$

$$\theta_2 = \frac{T(r,\tau) - T_0}{T_f - T_0} \quad \text{(Eq 6d)}$$

γ_n are the roots of:

$$\gamma_n J_1(\gamma_n) - \beta_c J_0(\gamma_n) = 0 \quad \text{(Eq 7)}$$

and β_c is the Biot number during cooling. above equations. Should they all be capitalized?

2.3 *Fundamental Equations for Stresses and Strains*

Total strains developed during heating of the cylinder are the sum of three terms—the elastic, thermal, and plastic components:

$$\varepsilon_{ij} = \varepsilon_{ij}^e = \partial_{ij}\int \alpha dT + \varepsilon_{ij}^p \quad \text{(Eq 8)}$$

During thermal cooling:

$$\varepsilon_{ij} = \varepsilon_{ij}^e + \partial_{ij}\int \alpha dT + \varepsilon_{ij}^p + \varepsilon_{ij}^R \quad \text{(Eq 8a)}$$

where ε_{ij}^R is the total strain accumulated during heating.

The following dimensionless parameters are defined as:

$$\sigma_r^* = \frac{(1-\nu)\sigma_r}{E_0\alpha_0(T_f - T_0)}$$

$$\varepsilon_r^* = \frac{(1-\nu)\varepsilon_r}{\alpha_0(T_f - T_0)}$$

$$B = B_1 \frac{E_0\alpha_0(T_f - T_0)}{(1-\nu)}$$

$$C = \frac{C_{11}}{[(T_f - T_0) + 273]} \qquad \text{(Eq 9)}$$

where the coefficient of thermal expansion α, the elastic modules E, and the yield stress σ_1 are assumed to be temperature dependent and have been defined in terms of two parameters:

$$\alpha = \alpha_0\alpha^*(\theta)$$

$$E = E_0E^*(\theta)$$

$$\sigma_1 = \sigma_{10}\sigma^*(\theta) \qquad \text{(Eq 10)}$$

and

$$\alpha^* = 1 + \alpha_1\theta$$

$$E^* = 1 - E_1\theta^2$$

$$\sigma_1^* = 1 + \sigma_{11}\theta + \sigma_{12}\theta^2 + \sigma_{13}\theta^3 \qquad \text{(Eq 11)}$$

Upon introducing these equations to the familiar stress-strain relation and substituting the results in the equilibrium and strain compatibility equations, one obtains:

$$E^*\varepsilon_\theta^* = \frac{1-2\nu}{2(1-\nu)}\int \varepsilon_\theta^* \frac{\partial E^*}{\partial \rho}\, d\rho + \frac{1}{2\rho^2(1-\nu)} \int \rho\varepsilon_\theta^* \frac{\partial E^*}{\partial \rho}\, d\rho + (1+\nu)\frac{1}{\rho^2}\int E^*\rho\left(\int \alpha^* d\theta\right)d\rho + \frac{1-2\nu}{2(1-\nu)}\int E^*(\varepsilon_r^{*p} - \varepsilon_\theta^{*p})\frac{d\rho}{\rho} + \frac{1-2\nu}{2\rho^2(1-\nu)}\int \rho E^* (\varepsilon_r^{*p} - \varepsilon_\theta^{*p})d\rho - \frac{\nu}{\rho^2(1-\nu)}\int \rho E^*\varepsilon_z^* d\rho + C_1 + \frac{C_2}{\rho^2} \qquad \text{(Eq 12)}$$

and

$$E^*\varepsilon_\theta^* = \frac{1-2\nu}{(1-\nu}\int \varepsilon_\theta^* \frac{\partial E^*}{\partial \rho}\, d\rho - E^*\varepsilon_\theta^* + (1+\nu)E^*\int \alpha^* d\theta + \frac{1-2\nu}{1-\nu}E^*\varepsilon_r^{*p} + \frac{1-2\nu}{1-\nu} \int \frac{E^*}{\rho}(\varepsilon_r^{*p} - \varepsilon_r^{*\theta})d\rho - \frac{\nu}{1-\nu}E^*\varepsilon_z^* + 2C_1 \qquad \text{(Eq 13)}$$

The boundary conditions are:

$$\sigma_r^*(\rho = 0) \neq \infty, \quad \sigma_r^*(\rho = 1) = 0, \quad 2\pi\int \sigma_z^*\rho d\rho = 0 \qquad \text{(Eq 14)}$$

By using the foregoing boundary conditions, the constants C_1 and C_2 and ε_z can easily be obtained:

$$C_2 = 0.0$$

$$C_1 = -\frac{(1-2\nu)}{2(1-\nu)}\left[\int_0^1 \varepsilon_\theta^* \frac{\partial E^*}{\partial \rho}\, d\rho - \int_0^1 \rho\varepsilon_\theta^* \frac{\partial E^*}{\partial \rho}\, d\rho + \int_0^1 E^*(\varepsilon_r^{*p} - \varepsilon_r^{*\theta})\frac{d\rho}{\rho} - (1-2\nu)\int_0^1 \rho E^*(\varepsilon_r^{*p} + \varepsilon_r^{*\theta})d\rho + 2\nu\int_0^1 \rho E^*\varepsilon_z^* d\rho - 2(1+\nu)(1-\nu)\int_0^1 \rho E^*\left(\int \alpha^* d\theta\right)d\rho\right] \qquad \text{(Eq 14a)}$$

$$\varepsilon_z^* = \left(\frac{1}{\int_0^1 E^*\rho d\rho}\right)\left[(1-\nu)\int_0^1 E^*\left(\int \alpha^* d\theta\right)\rho d\rho - \int_0^1 \rho E^*(\varepsilon_\theta^{*p} + \varepsilon_r^{*p})d\rho\right] \qquad \text{(Eq 14b)}$$

2.4 *Plastic Strain Increment*

The plastic strains that are parts of Eq 12 and 13 can be evaluated using the following:

$$\varepsilon_{ij}^{*p} = \varepsilon_{ij}^{*n}(r,t) + \dot{\varepsilon}_{ij}^{*(n)}(r,t)\Delta\tau \qquad \text{(Eq 15)}$$

where the hyperbolic sine law of Tine et al. (Ref 27, 28) was adopted for the plastic strain increment:

$$\dot{\varepsilon}_{ii}^{(n)} = \frac{3}{2}Ae^{-C/\theta}\{[\sinh(B\sigma)]^n/\sigma\}s_{ii}$$

$$\sigma = \sqrt{\frac{3}{2}(S_{rr}^2 + S_{\theta\theta}^2 + S_{zz}^2} \qquad \text{(Eq 16)}$$

(no sum over i), where A, B, and C are material parameters and are assumed to be constant.

3. Numerical Procedure

The following procedure was adopted for the numerical analysis. Initially, the cross section of the cylinder was partitioned into 100 unequal elements in the radial direction, and the time increments were divided into 50 unequal parts. The radial divisions at areas closer to the outer surfaces and the time increments at the early stage of cooling were smaller than the other divisions. At those areas or during those time intervals, the material experiences a more rapid temperature gradient.

At time t, a first approximation for strains was obtained using Eq 12 and 13 and assuming the tangential strains in the right sides of the equations to be zero. Subsequently, the value of ε_θ^* on the right side of Eq 12 and 13 is the first initialized value of ε_θ^* at time t. The new value is used to obtain a better value for ε_θ^*. This procedure is repeated until a desired convergency is obtained. Equation 16 was used to obtain the plastic strains; σ was evaluated using the stresses at step $(i-1)$. Having new values for strains, one can easily obtain the new stresses and a new value for strain rate. From this value, the new plastic strain is estimated by modifying the scheme outlined in Ref 29 and 30. The corrected value of the plastic strain, $\dot{\varepsilon}_{ij}^{(n)c}$, is evaluated using the following:

$$\varepsilon_{ij}^{(p)c} = \varepsilon_{ij}^{p}(r,t) + \frac{\Delta\tau}{2}\left[\dot{\varepsilon}_{ij}^{(n)c} + \dot{\varepsilon}_{ij}^{(n)}\right] \quad \text{(Eq 17)}$$

Having the plastic strains, a total effective strain can be defined as follows:

$$\varepsilon_e = \sqrt{\frac{2}{3}\varepsilon_{ij}\varepsilon_{ij}}$$
$$\varepsilon_e^c = \sqrt{\frac{2}{3}\varepsilon_{ij}^c\varepsilon_{ij}^c} \quad \text{(Eq 18)}$$

The maximum relative difference between the effective strain and the corrected strain was found. If it lay within a prescribed error tolerance, it was accepted; otherwise, the procedure was repeated until a desired convergency was reached.

In this analysis, $\Delta\tau$ must be small enough to prevent overshooting of stresses, which was accomplished using the following procedure. During loading and unloading of the cylinder (here, unloading refers to situations where elastic stresses are released), whether the stresses are compressive or tensile, one can easily show that the following conditions always apply:

- $\left|\Delta\varepsilon_{ij}^{p}\right| < \left|\Delta\varepsilon_{ij}^{(\text{total})}\right|$.
- $\Delta\varepsilon_{ij}^{e+p+th}$ and $\Delta\varepsilon_{ij}^{p}$ should be of the same sign.
- S_{ij} and $\Delta\varepsilon_{ij}^{p}$ should be of the same sign.

Accordingly, at each time step the above conditions were checked before accepting the strain increment. If the conditions were not satisfied, the time increment was locally divided into 10 smaller increments and the same procedure followed.

3.1 *Results of Numerical Calculation*

For the purposes of discussion and comparison with experimental results, the following data for steel containing 0.3% C, 0.2% Si, 0.45% Mn, 1.3% Cr, and 4.45% Ni were used (Ref 27, 28, 31):

$$K_0 = 59.7\ \text{W/m} \cdot \text{K}$$
$$E_0 = 206.0 \times 10^9\ \text{N/m}^2$$
$$\sigma_{10} = 295 \times 10^6\ \text{N/m}^2$$
$$\sigma_{12} = -5.50 \times 10^{-3}\lambda^2$$
$$K_1 = 0.0334\lambda \quad \text{(Eq 19)}$$

$$E_1 = 2.34 \times 10^{-3}\lambda^2$$
$$\sigma_{11} = 0.017\lambda$$
$$T_f = 840\ ^\circ\text{C}$$
$$T_0 = 0.0\ ^\circ\text{C}$$
$$\sigma_{13} = 2.53 \times 10^{-4}\lambda^4 \quad \text{(Eq 20)}$$

where λ is called the loading parameter and is defined as:

$$\lambda = \frac{E_0\alpha_0 T_0}{(1-\nu)\sigma_0} \quad \text{(Eq 21)}$$

The results in this paper are for $\lambda = 6$, and the Poisson ratio ($\nu = 0.4$) is assumed to be unaffected by temperature (Ref 16-20).

3.2 *Coefficient of Thermal Expansion*

The coefficient of thermal expansion changes with temperature (Ref 16-20). However, the change during phase transformation is far greater. The following data (Ref 16, 27, 28, 31) were used:

During heating:

$$\alpha_0 = 1.47 \times 10^{-5}\,\text{C}^{-1},\ \alpha_1 = 1.0 \quad \text{for } 0 < \theta < 0.866$$
$$\alpha_0 = -3.22 \times 10^{-5}\,\text{C}^{-1},\ \alpha_1 = -2.19 \quad \text{for } 0.866 \le \theta < 0.988$$
$$\alpha_0 = 1.97 \times 10^{-5}\,\text{C}^{-1},\ \alpha_1 = 1.34 \quad \text{for } 0.988 \le \theta \le 1.0 \quad \text{(Eq 22)}$$

where the minus sign corresponds to volumetric change.

During rapid cooling:

$$\alpha_0 = 1.12 \times 10^{-8}\,\text{C}^{-1},\ \alpha_1 = 1.34 \quad \text{for } 0.605 > \theta \ge 0$$
$$\alpha_0 = 1.97 \times 10^{-5}\,\text{C}^{-1},\ \alpha_1 = 7.63 \times 10^{-4} \quad \text{for } 0.605 < \theta \le 1.0 \quad \text{(Eq 23)}$$

For the portion of the cylinder whose temperature remained under the critical temperature, the following data were used:

$$\alpha_0 = 1.47 \times 10^{-5}\,\text{C}^{-1},\ \alpha_1 = 1.0 \quad \text{(Eq 24)}$$

4. Discussion

Figures 3 and 4 show the temperature distribution during rapid heating and rapid cooling, respectively. At $t = 0.176$, the cylinder was rapidly cooled. As is clear, only a very small portion of the cylinder at the vicinity of the surface passed the critical temperature. Figures 5 and 6 show the tangential and longitudinal stresses, respectively, at the surface of the cylinder

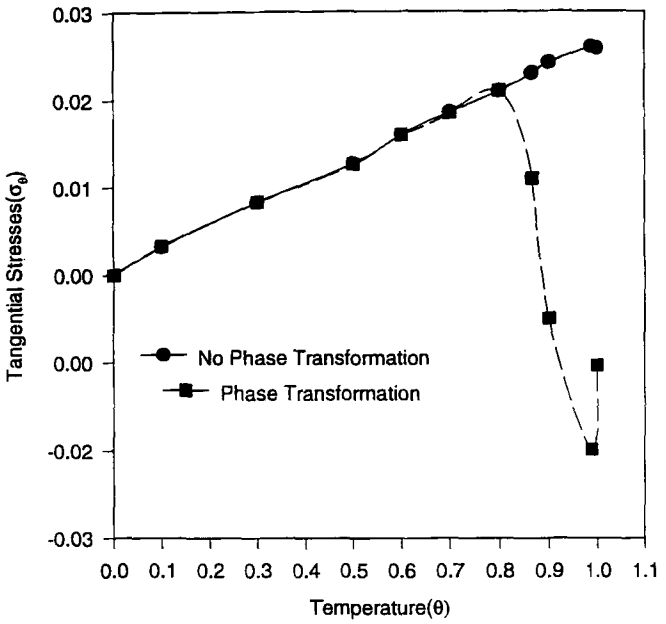

Fig. 5 Tangential stresses at the surface of the cylinder during heating

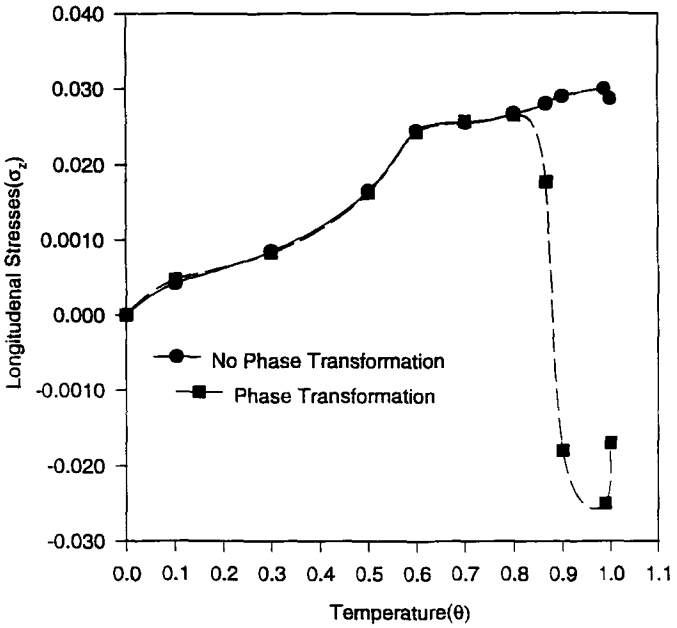

Fig. 6 Longitudinal stresses at the surface of the cylinder during heating

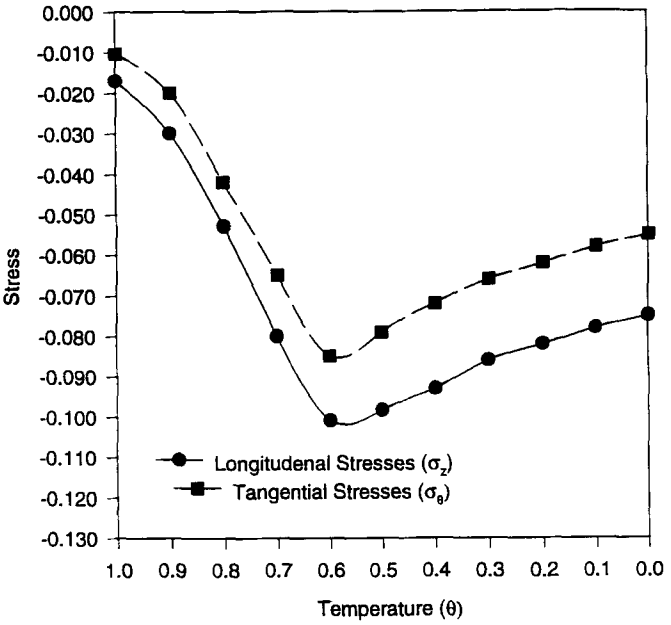

Fig. 7 Thermoelastoplastic stresses at the surface of the cylinder during cooling

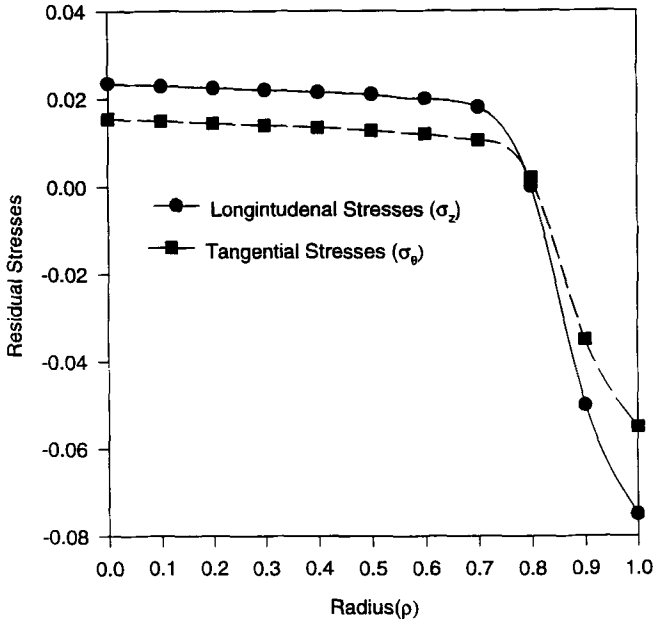

Fig. 8 Residual stress distribution

during heating. As shown, by neglecting the phase transformation, the results are overestimated. Careful scrutiny of these results indicates that as the temperature gradient increases, tensile stresses develop and increase at the surface of the cylinder. However, at $\theta = 0.86$ they suddenly decrease and even become compressive. During the later stages of heating, the stresses again show an increasing trend. This is because as the temperature increases, the cylinder expands regularly. Once the temperature passes 723 °C, phase transformation occurs and the cylinder begins to contract. During heating through the range from 723 to 830 °C, α-iron transforms to γ-iron, and iron carbide goes into solution in γ-iron. At 830 °C steel resumes its expansion. When phase transformation is not considered in numerical simulation, the increasing trend of stresses continues.

If the cooling rate is high enough during the cooling of low-carbon steel, the formation of pearlite and bainite is avoided,

and martensite is produced (Fig. 2). During this process, austenite is completely transformed to martensite. Figure 7 depicts the tangential and longitudinal stresses at the surface of the cylinder during rapid cooling. The curves indicate that compressive stresses develop up to a temperature of $\theta = 0.605$; then tensile stresses develop. The curves have a decreasing trend up to $\theta = 0.605$. Beyond this temperature, the stress suddenly assumes an increasing trend (tensile stresses are developed). This can be explained as follows. When the cylinder is rapidly cooled, as discussed earlier, formation of pearlite and bainite is avoided (due to the high rate of cooling). Accordingly, the trend of the curve at temperatures of 723 and 830 °C, which are equivalent to $\theta = 0.866$ and 0.988, respectively, does not change. However, at $\theta = 0.605$ martensite transformation occurs and suddenly the trend of the curve begins to increase. During cooling, the cylinder contracts regularly; however, once martensite transformation occurs, it begins to expand. This results in the trend depicted in Fig. 7. Figure 8 shows the residual stresses across the radius of the cylinder. The magnitude of stresses at the vicinity of the surface is higher than at the center, because the rate of cooling near the surface is higher than at the center.

5. Conclusions

The stresses developed in a solid cylinder during induction hardening has been evaluated and the following conclusions derived from the results:

- Phase transformation is an important factor in evaluating residual stresses during induction hardening.
- By rapid heating and cooling the cylinder, the level of beneficial residual stresses at the surface becomes considerably higher than the tensile residual stresses at the center.

Nomenclature

a	radius of cylinder, m
C	specific heat, kJ/kg · K
E	Young's modulus, N/m^2
K	thermal conductivity, W/m · K
t	time, s
α	coefficient of thermal expansion, °C^{-1}
γ	mass density, kg/m^{-3}
ε_{ij}	total strain tensor
θ	dimensionless temperature
ν	Poisson's ratio (0.3)
ρ	dimensionless radius
σ_{10}	yield stress, psi (N/m^2)
σ_i	total stress tensor, N/m^2
τ	dimensionless time

References

1. G. Sachs, Der Nachweis Inneres Spannungen in Stangen Und Rohren, *Z. Metallkd.*, Vol 19, 1927, p 352 (in German)
2. J.H. Weiner and J.V. Huddleston, Transient and Residual Stresses in Heat-Treated Cylinders, *J. Appl. Mech. (Trans. ASME)*, Vol 26, March 1959, p 31-39
3. H.G. Landu and J.H. Weiner, Stresses in an Elastic-Plastic Cylinder due to a Dilatational Phase Transformation, *J. Appl. Mech. (Trans. ASME)* Ser E 31, 1964, p 148-150
4. C. Hwang, Thermal Stresses in an Elastic, Work-Hardening Sphere, *J. Appl. Mech. Trans. ASME)*, Dec 1960, p 629-634
5. S. Chu, A Numerical Thermoelastoplastic Solution of a Thick-Walled Tube, *AIAA J.*, Vol 12 (No. 2), 1974, p 176-179
6. V. Sagar and D.J. Payne, Elasto-plastic Deformations of Thick-walled Circular Cylinders under Transient Heating and Combined Axial Tension and Torsion Loads, *J. Mech. Phys. Solids*, Vol 22, 1974, p 47-59
7. S. Weirzbinski, The Strain Hardening of Copper Carbon after Rapid Continuous Heating, *Phys. Met. Metallogr. (USSR)*, Vol 59 (No. 6), 1985, p 148-153
8. Y.N. Shevchenko, S.V. Novikov, and A.Z. Galishin, Determination of the Thermoelastoplastic Stress-Strain State of Cylinder Tubes with Corrugated Inserts, *Sov. Appl. Mech.*, Vol 27 (No. 8), Feb 1992, p 785-793
9. N.I. Kabasko, Increasing the Service Life of Machine Parts and Tools by Intensification of Cooling of Them in Quenching, *Met. Sci. Heat Treat.*, Vol 28 (No. 9/10), Sept/Oct 1986, p 758-764
10. A.R. Gachkevich and V.Ya. Boinchuck, Thermal Stresses of a Long Cylinder Heated by Thermal Radiation, *Sov. Appl. Mech.*, Vol 23 (No. 4), April 1987, p 328-332
11. J.R. Thomas, Jr., J.P. Singh, H. Tawil, and L. Powers, Thermal Stresses in a Long Circular Cylinder Subjected to Sudden Cooling during Transient Convection Heating, *J. Therm. Stress.*, Vol 8, 1985, p 249-260
12. A. Mendelson, *Plasticity: Theory and Application*, Macmillan, 1968, p 98-133
13. H. Ishikawa, Transient Thermoelastoplastic Stress Analysis for a Hollow Sphere Using Incremental Theory of Plasticity, *Int. J. Solids Struct.*, Vol 13, 1977, p 645-655
14. H. Ishikawa, A Thermoelastoplastic Solution for a Circular Solid Cylinder Subjected to Heating and Cooling, *J. Therm. Stress.*, Vol 1, 1978, p 211-222
15. H. Ishikawa and K. Hata, Thermoelastoplastic Creep Stress Analysis for a Thick-Walled Tube, *Int. J. Solids Struct.*, Vol 16, 1980, p 291-299
16. H. Ishikawa, Y. Sugawara, and K. Hata, Thermoelastoplastic Stress Analysis during Phase Transformation, *J. Therm. Stress.*, Vol 6, 1983, p 365-377
17. S. Jahanian and M. Sabbaghian, Thermoelastoplastic and Residual Stresses in a Hollow Cylinder with Temperature-Dependent Properties, *J. Pressure Vessel Technol. (Trans. ASME)*, Vol 112, Feb 1990, p 85-91
18. S. Jahanian and M. Sabbaghian, Residual Stresses in A Hollow Cylinder due to Rapid Cooling of Casting, *Design and Analysis of Piping, Pressure Vessels, and Components*, PVP-Vol 120, American Society of Mechanical Engineering, 1987, p 155-163
19. S. Jahanian, Plastic Deformation of a Thick-Walled Circular Cylinder with Temperature Dependent Properties under Transient Heating and Combined Axial and Torsion Load, *Reliability, Stress Analysis, ad Failure Prevention Aspects of Composite and Active Materials*, DE-Vol. 79, American Society of Mechanical Engineering, 1993, p 55-64
20. S. Jahanian, Determination of Residual Stress Distribution in Sensitive and Insensitive Materials, *Reliability, Stress Analysis, and Failure Prevention*, DE-Vol 55, American Society of Mechanical Engineering, 1993, p 179-183
21. M. Mitter, F.G. Rammerstorfer, and O. Grundler, Discrepancies between Calculated and Measured Residual Stresses in Quenched Pure Iron Cylinder, *Mater. Sci. Technol.*, Vol 1, Oct 1985, p 793-797

22. F.G. Rammerstorfer, D.F. Fischer, W. Mitter, K.J. Bathe, and M.D. Snyder, On Thermoelastoplastic Analysis of Heat Treatment Process Including Creep and Phase Transformation, *Comput. Struct.*, Vol 13, 1981, p 771-779
23. H.R. Tien and O. Richmond, Theory of Maximum Tensile Stresses in the Solidifying Shell of a Constrained Rectangular Casting, *J. Appl. Mech. (Trans. ASME)*, Vol 49, 1982, p 481-486
24. S.L. Semiatin, *Induction Heat Treatment of Steel*, ASM International, 1986, p 10
25. C.R. Brooks, *Heat Treatment of Ferrous Alloys*, Hemisphere Publishing, 1979, p 44
26. H.S. Carslaw and J.C. Jeager, *Conduction of Heat in Solids*, 2nd ed., Oxford University Press, 1980
27. G.V. Smith, *An Evaluation of the Elevated Temperature Tensile and Creep-Rupture Properties of Wrought Carbon Steel*, DS11S1, ASTM, 1970, p 27
28. *Metals Handbook*, Vol 1, 9th ed., American Society for Metals, 1979, p 653
29. N. Zabaras, S. Mukherjee, and W.R. Arthur, A Numerical and Experimental Study of Quenching of Circular Cylinders, *J. Therm. Stresses*, Vol 10, 1987, p 177-191
30. S. Mukherjee, *Boundary Element Methods in Creep and Fracture*, Applied Science Publishers, 1982, p 39
31. C.S. Barrett and T.B. Massalski, *Structure of Metals*, 3rd ed., McGraw-Hill, 1966, p 511